Mechanistic study of reaction mechanism on ammonia photodecomposition over Ni/TiO$_2$ photocatalysts

Arisa Utsunomiya [a], Atsushi Okemoto [a], Yukihiro Nishino [a], Kensuke Kitagawa [a], Hisayoshi Kobayashi [b], Keita Taniya [a], Yuichi Ichihashi [a,*], Satoru Nishiyama [a]

[a] Department of Chemical Science and Engineering, Graduate School of Engineering, Kobe University, Rokkodaicho 1-1, Nada, Kobe, 657-8501, Japan
[b] Department of Chemistry and Materials Technology, Kyoto Institute of Technology, Matsugasaki, Sakyou-ku, Kyoto, 606-8585, Japan

ABSTRACT

Photodecomposition of NH$_3$ to H$_2$ and N$_2$ was carried out using metal-supported TiO$_2$ (M/TiO$_2$) photo-catalysts in an aqueous NH$_3$ solution under UV irradiation at room temperature. Ni/TiO$_2$ photocatalysts indicated the highest yield of H$_2$. The NH$_2$ radical was formed as a dominant intermediate during NH$_3$ decomposition, as confirmed by electron spin resonance measurements. Reaction pathways via NH$_2$ radical formation were also investigated in detail by density functional theory. The results showed that H$_2$ and the H$_2$N-NH$_2$ as intermediate were formed by the coupling of an NH$_2$ radical and an NH$_3$ molecule in the gas phase during the photodecomposition of NH$_3$. We believe that our findings would be useful for further developing efficient catalytic systems.

© 2017 Elsevier B.V. All rights reserved.

1. Introduction

Photocatalytic reactions have been widely investigated owing to their potential applications in environmental cleaning and energy generation, because of increasing concerns about environmental issues and energy demands caused by the consumption of nonrenewable fossil fuels [1–6]. One such photocatalytic process involves producing H$_2$ as an energy resource and is expected to be both economically and environmentally friendly as well as contribute to the establishment of a H$_2$ production method for obtaining renewable energy [4,5,7,8].

Very little elemental hydrogen exists in the Earth's atmosphere. H$_2$ is produced from hydrogen-containing compounds [9]. Photocatalytic splitting of water has been considered an excellent alternative source of energy since Fujishima and Honda reported the potential use of titanium dioxide (TiO$_2$) as a photoelectrode for water electrolysis to produce O$_2$ and H$_2$ [1,6]. Recently, NH$_3$ has been utilized in many efforts to develop a technology for the storage and supply of H$_2$ [9,10]. NH$_3$ has a high energy density and a high H$_2$ storage capacity of 17.6 wt% in comparison with other carriers such as cyclohexane, ethanol, and liquefied petroleum gas (LPG).

Moreover, NH$_3$ decomposition does not produce CO$_2$ because it is a no carbon compound. NH$_3$ can be easily stored and transported in the liquid phase because NH$_3$ gas is liquefied under a pressure of 8.5 MPa at 20 °C. NH$_3$ photodecomposition has also attracted much attention because of its milder reaction conditions and its lower environmental burden than that of thermal decomposition processes [11–15]. Thus, photocatalytic reactions for H$_2$ production in an aqueous NH$_3$ solution are highly useful and constitute a fascinating area of research.

TiO$_2$ is the most popular materials for photocatalysis because of its low price, high availability, high chemical stability, low toxicity, and excellent light conversion efficiency [16–23]. TiO$_2$ is an indirect bandgap semiconductor with a bandgap of 3.2 eV. TiO$_2$ has good optical properties and shows photocatalytic activity in the UV region [24–26]. However, its photocatalytic efficiency is still relatively low because of the fast recombination of the photoinduced charge carriers. Many studies have reported improved photocatalytic efficiency of TiO$_2$ by doping with a second component such as Fe and Cr, which promotes the photon-to-electron conversion efficiency and charge separation [15,25]. Our group has recently demonstrated that loading Pt on an Fe-doped TiO$_2$ photocatalyst results in a higher activity for H$_2$ production by NH$_3$ decomposition [15]. However, to the best our knowledge, the mechanism of NH$_3$ decomposition is still not well understood [12–15]. Quantum chemical calculations can effectively reveal the microcosmic mechanisms of complex chemical reactions and provide information about changes in the structure and chemical reaction energy

* Corresponding author at: Department of Chemical Science and Engineering, Graduate School of Engineering, Kobe University, Rokkodaicho 1-1, Nada, Kobe, 657-8501, Japan.
E-mail address: ichiy@kobe-u.ac.jp (Y. Ichihashi).

as a consequence of such reactions [27]. They can also aid in further developments of efficient catalytic systems.

In this study, an attempt is made to produce H_2 by decomposition of NH_3 catalyzed by TiO_2 photocatalysts. Theoretical calculations and the experiments designed to further probe the mechanisms of these reactions are performed. Finally, we proposed a reasonable reaction mechanism using a combination of electron spin resonance (ESR) measurements and density functional theory (DFT) calculations [28–34].

2. Experimental

2.1. Catalyst preparation

Metal-loaded TiO_2 (JRC-TIO-4, Catalysis Society of Japan) photocatalysts (M/TiO_2, where $M = V$, Cr, Mn, Fe, Co, Cu, Zn, and Pt) were prepared by an impregnation method using an aqueous solution of $Ni(NO)_3 \cdot 6H_2O$ (0.26 g; Nacalai Tesque) in deionized water (50 mL). TiO_2 (1.00 g) was added into the aqueous solution in which the precursor was dissolved. The precursors were NH_4VO_3, $Cr(NO_3)_2 \cdot 6H_2O$, $Mn(NO_3)_2 \cdot 6H_2O$, $Fe(NO_3)_3 \cdot 9H_2O$, $CoCl_2 \cdot 6H_2O$, $Cu(NO_3)_2 \cdot 3H_2O$, $Zn(NO_3)_2 \cdot 6H_2O$ (all supplied by Nacalai Tesque), and H_2PtCl_6 (Tanaka Kikinzoku Kogyo). The solvent was evaporated from the mixture obtained in vacuum at 353 K, and then the solid obtained was dried in vacuum at room temperature overnight. The obtained powder was calcined in air at 723 K for 5 h, and then reduced by hydrogen at 723 K for 3 h. The solid thus acquired was designated as 0.5 wt% M/TiO_2.

2.2. Photocatalytic decomposition of NH_3

Hydrogen production from the photocatalytic decomposition of NH_3 was performed in a 8 mL quartz-glass batch reactor. The catalyst (20 mg) and an aqueous ammonia solution (5 mL, 0.59 mol/L) were charged into the reactor. The reactor was purged with Ar gas for 20 min to remove air completely. The reaction solution was then magnetically stirred under irradiation using a Xe lamp (500 W) through a color filter (Hoya UV-25) for 3 h. The gas-phase products were analyzed by gas chromatography (GC, Shimadzu GC-8A) equipped with a thermal conductivity detector using Ar carrier gas and by mass spectrometry (MS) using a quadrupole mass spectrometer (QME220).

2.3. Characterization

Powder X-ray diffraction (XRD) measurements were performed using a Rigaku RINT-2100 system with Cu Kα radiation ($\lambda = 1.5406$ Å). ESR data were recorded using an X-band spectrometer (Bruker ESR 300E). The following experimental procedure was followed for the photocomposition of NH_3: the catalyst was placed into a glass cell with a quartz ESR cell and an attached 3-way stop valve. The cell was charged with H_2 (100 Torr), heated at 623 K for 30 min, and then evacuated at room temperature to remove H_2 completely. The reduced sample was transferred into the ESR cell, followed by the introduction of gaseous NH_3 (110 Torr) for absorbing NH_3 to the sample surface. NH_3 charged in the cell was then evacuated until the pressure inside decreased to less than 3 Torr. The ESR spectrum was recorded at 77 K under UV light irradiation.

2.4. Computational methods

The calculation model is shown in Fig. 1 [35–37]. DFT calculations were performed using the Gaussian 03 package. All calculations used the spin-unrestricted hybrid density functional B3LYP and the basis set LanL2DZ; molecular geometries of all the structures were fully optimized. The calculations were performed
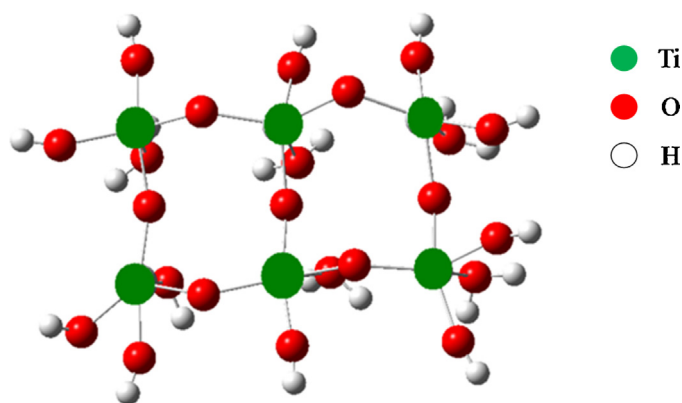

Fig. 1. TiO_2 cluster used as calculation model.

Table 1
Yield of H_2 on NH_3 photodecomposition over 0.5 wt% M/TiO_2 (Irradiation time: 3 h).

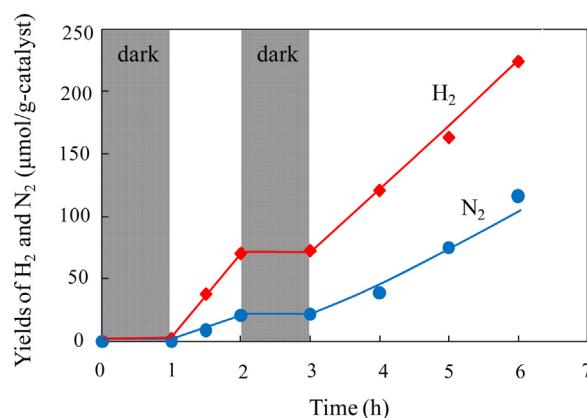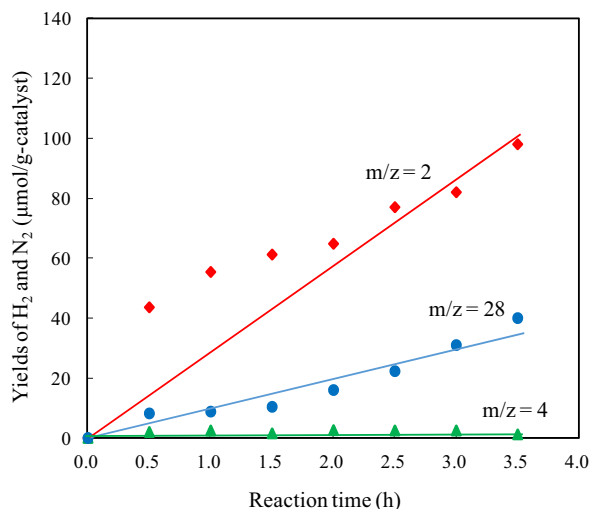| Entry no.	Catalysts	Yield of H_2 (μmol/g-cat)
1	TiO_2	8.7
2	V/TiO_2	6.0
3	Cr/TiO_2	7.0
4	Mn/TiO_2	7.2
5	Fe/TiO_2	6.7
6	Co/TiO_2	6.3
7	Cu/TiO_2	6.8
8	Ni/TiO_2	131.7
9	Ni/TiO_2[a]	8.4

[a] Without H_2 reduction.

Fig. 2. Time profiles of H_2 and N_2 yields for the NH_3 photodecomposition over Ni/TiO_2.

using the triplet excited state (spin = triplet) to account for TiO_2 photoexcitation [38].
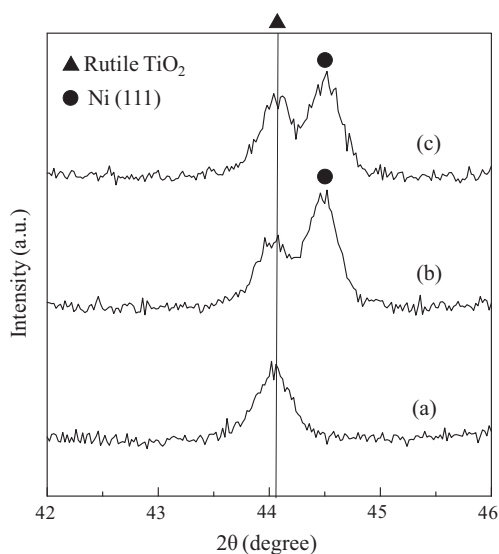
3. Results and discussion

3.1. Photocatalytic decomposition of NH_3

Photocatalytic H_2 production from NH_3 over the as-prepared TiO_2 catalysts loaded with various metals (M/TiO_2) was evaluated under UV irradiation in an aqueous NH_3 solution at room temperature (see Table 1). H_2 was obtained in a yield of 8.7 μmol/g-catalyst over pure TiO_2 (Entry 1). Photocatalytic activities of TiO_2 catalysts loaded with several transition metals except for Ni were almost equal to that of pure TiO_2 (Entries 2–7). However, Ni/TiO_2 effectively enhanced H_2 formation (Entry 8). The time profiles of H_2 and N_2 yields in the NH_3 (aq.) decomposition over Ni/TiO_2 are shown in Fig. 2. No formation of H_2 and N_2 was observed in the dark.

Fig. 3. Time profiles of products yields for the NH_3 photodecomposition over Ni/TiO_2 (1.0 wt%) in gas phase reaction (Reactant: $NH_3 + D_2O$).
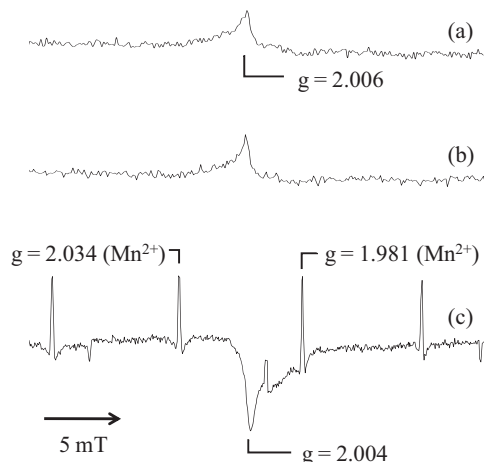

Fig. 5. ESR spectra of Ni/TiO_2 (a), NH_3 absorption without photoirradiation (b), and under photoirradiation (c)(NH_3 3 Torr, at 77 K).

Fig. 4. XRD patterns of TiO_2 (a), Ni/TiO_2 before the reaction (b) and Ni/TiO_2 after the reaction (c).

Fig. 6. Energy diagram for the NH_3 decomposition to N_2 and H_2 in pathway route 1 over TiO_2 photocatalyst.
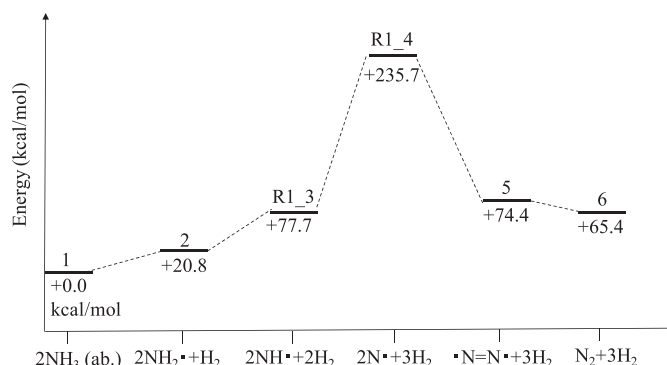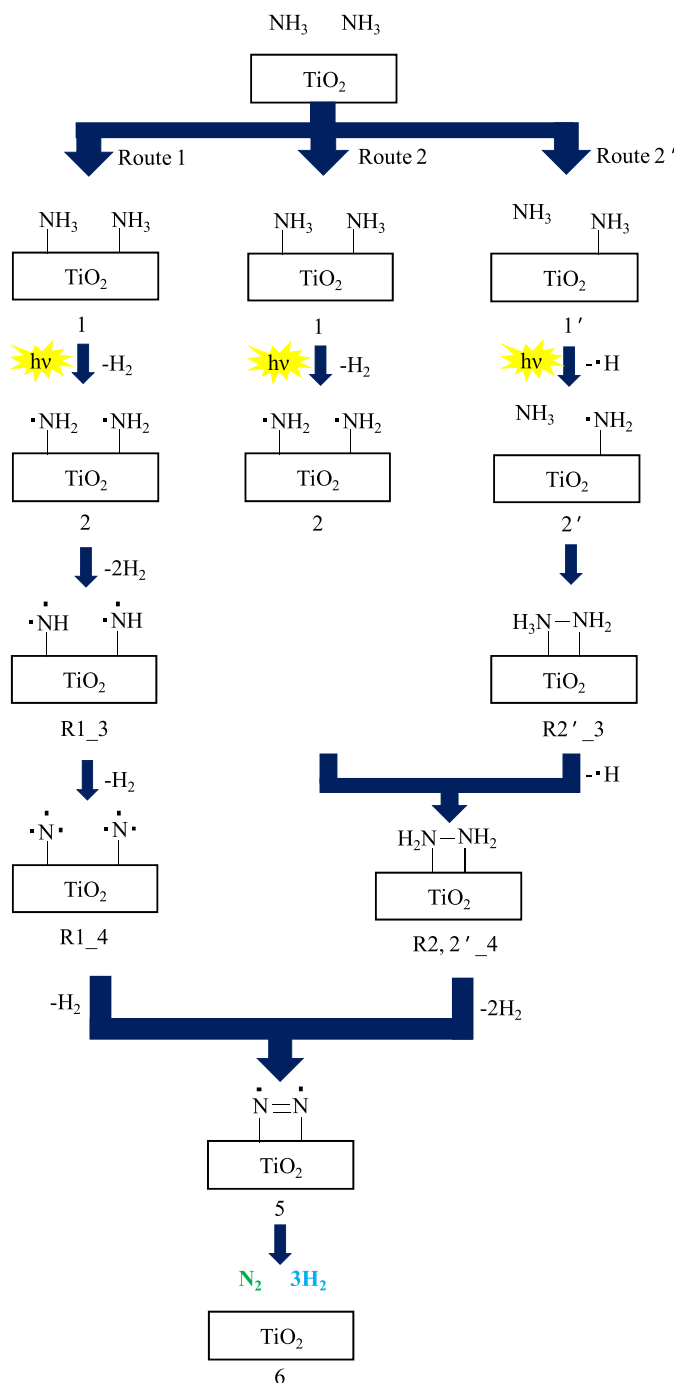
UV light irradiation caused H_2 and N_2 production, and the yields increased linearly with the reaction time. H_2 and N_2 were found to be produced in a 1:3 molar ratio, indicating they are produced stoichiometrically owing to NH_3 photodecomposition. It was also confirmed that hydrogen was formed because of NH_3 decomposition with the aid MS using D_2O. As shown in Fig. 3, the signal for H_2 ($m/z = 2$) was observed for NH_3 decomposition in D_2O, but the signal for D_2 ($m/z = 4$) was not, implying that the H_2 formed was derived from the photodecomposition of NH_3.

3.2. Characterization of Ni/TiO_2

XRD patterns of both TiO_2 and Ni/TiO_2 before and after the reaction are shown in Fig. 4(b) and (c), respectively. Fig. 4(c) shows a similar diffraction pattern as that of Fig. 4(b). The peaks at $2\theta = 44.5°$ and $44.1°$ were assigned to Ni^0 (111) and rutile TiO_2, respectively [39–44]. This indicates that the crystal structures of TiO_2 and Ni metal are stable during the reaction of NH_3 in an aqueous solution. It also suggests that Ni^0 on TiO_2 enhances the NH_3 decomposi-

tion because Ni^{00} was present in the catalyst that showed a higher catalytic activity than the others (see Table 1, Entries 8 and 9).

3.3. Reaction mechanism of NH_3 decomposition over TiO_2 photocatalyst

ESR measurements were employed to observe the formation of intermediates during the NH_3 decomposition reaction. The ESR spectra of Ni/TiO_2 are shown in Fig. 5. Fig. 5(a) and (b) are the spectra for Ni/TiO_2 and the catalyst adsorbed NH_3, respectively. The spectra exhibit a signal at $g = 2.006$, which was assigned to TiO_2 [45]. The spectrum in Fig. 5(c), obtained during UV irradiation, shows a signal at $g = 2.004$ that was assigned to the NH_2 radical [46,47]. The ESR measurement results indicated that the NH_2 radical was formed as a dominant intermediate from NH_3 photodecomposition. It was suggested that the NH_2 radical was formed by the extraction of a hydrogen atom from NH_3. To further investigate the reaction pathways in which H_2 and N_2 could be formed from NH_2 radicals, three pathways were proposed: route 1, route 2, and route 2′ (see Scheme 1). The Gibbs free energy was estimated for each elementary step of the three reaction pathways (see Figs. 6–8). NH_3 adsorption to the TiO_2 surface was considered the first step for each pathway. The adsorption of two molecules of NH_3 to the TiO_2 surface was an exothermic step with an associated enthalpy change of -7.4 kcal/mol.

NH$_3$ NH$_3$

| TiO$_2$ |

Route 1   Route 2   Route 2 ′

NH$_3$ NH$_3$ NH$_3$ NH$_3$ NH$_3$ NH$_3$

| TiO$_2$ | | TiO$_2$ | | TiO$_2$ |

1   1   1 ′

hν, -H$_2$ hν, -H$_2$ hν, -·H

·NH$_2$ ·NH$_2$ ·NH$_2$ ·NH$_2$ NH$_3$ ·NH$_2$

| TiO$_2$ | | TiO$_2$ | | TiO$_2$ |

2   2   2 ′

-2H$_2$

·N̈H ·N̈H   H$_3$N—NH$_2$

| TiO$_2$ | | TiO$_2$ |

R1_3   R2′_3

-H$_2$ -·H

·N̈· ·N̈·   H$_2$N—NH$_2$

| TiO$_2$ | | TiO$_2$ |

R1_4   R2, 2′_4

-H$_2$ -2H$_2$

N̈=N̈

| TiO$_2$ |

5

N$_2$ 3H$_2$

| TiO$_2$ |

6

Scheme 1. Suggested reaction mechanism for NH$_3$ decomposition to N$_2$ and H$_2$ over TiO$_2$ photocatalyst.

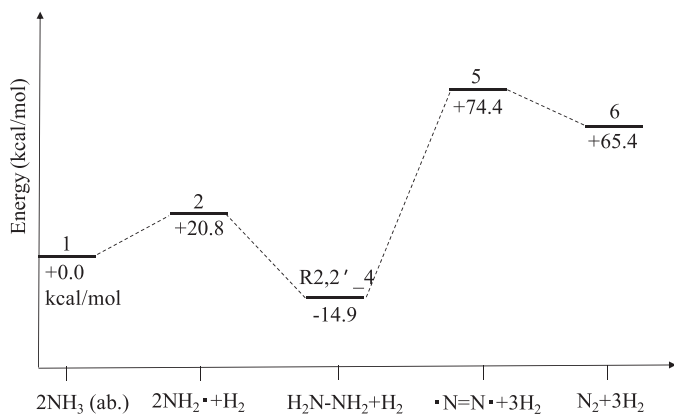### 3.3.1. Energy profile of route 1

Route 1 is the reaction pathway that generates the NH radical through extraction of two H atoms from NH$_3$ (Scheme 1). Fig. 6 shows the energy diagram for the steps of route 1, from NH$_3$ adsorption to the formation of N$_2$ and H$_2$. The NH$_2$ radical is formed through extraction of one H atom from the NH$_3$ adsorbed on TiO$_2$: this step is energetically 20.8 kcal/mol higher than the state of adsorbed NH$_3$ ($1 \rightarrow 2$). Next, H$_2$ desorption to form the NH radicals occurs by the extraction of one hydrogen atom from each of two NH$_2$ radicals. The step of NH radical formation from the NH$_2$ radical requires 77.7 kcal/mol of energy ($2 \rightarrow R1\_3$). The N radical is formed through the extraction of the H atom from the NH radical and is at the highest energy level in route 1 ($R1\_3 \rightarrow R1\_4$). The
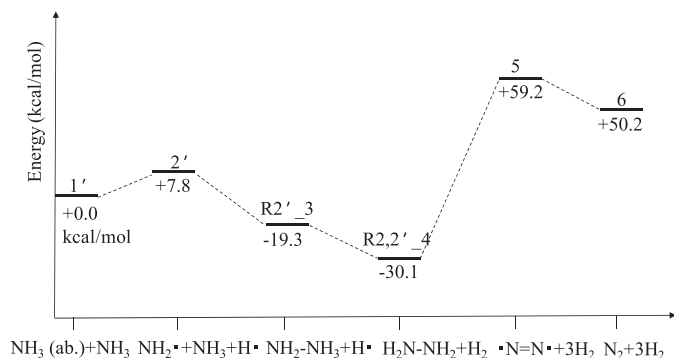
coupling of N radicals gives N$_2$ ($R1\_4 \rightarrow 5 \rightarrow 6$). In summary, the activation energy for H$_2$ and N$_2$ formation from NH$_3$ decomposition according to route 1 is estimated to be 236 kcal/mol.

3.3.2. Energy profile of route 2

In route 2, NH$_3$ photodecomposition occurs via the formation of H$_2$N-NH$_2$, which is formed by the coupling of adjacent NH$_2$ radicals (see Scheme 1). Fig. 7 shows the energy diagram for all the steps, from NH$_3$ adsorption to N$_2$ and H$_2$ formation, for route 2. The NH$_2$ radical is formed through the extraction of H atom from the NH$_3$ adsorbed on TiO$_2$ ($1 \rightarrow 2$). The coupling of adjacent NH$_2$ radicals gives H$_2$N-NH$_2$, and is an exothermic step with an enthalpy change of -14.9 kcal/mol ($2 \rightarrow R2,2'\_4$). The N=N radical is produced

Fig. 7. Energy diagram for the NH_3 decomposition to N_2 and H_2 in pathway route 2 over TiO_2 photocatalyst.

Fig. 8. Energy diagram for the NH_3 decomposition to N_2 and H_2 in pathway route 2 ′ over TiO_2 photocatalyst.

through the extraction of two hydrogen molecules from H_2N-NH_2: this step requires 74.4 kcal/mol of energy ($R2,2'\_4 \rightarrow 5$). N_2 is then obtained from the N=N radical as in route 1 ($5 \rightarrow 6$). The N=N radical is at the highest energy level in route 2. The activation energy of NH_3 decomposition to H_2 and N_2 according to route 2 is estimated to be 74.4 kcal/mol.

3.3.3. *Energy profile of route 2′*

Route 2′ is the reaction pathway where NH_3 photodecomposition occurs via H_2N-NH_2 formation, during which one NH_2 radical reacts with NH_3 in the gas phase (see Scheme 1). Fig. 8 shows the energy diagram for the steps of the pathway proposed by route 2′. The NH_2 radical is formed through extraction of a H atom from the NH_3 adsorbed on TiO_2, which is associated to an enthalpy change of 23.4 kcal/mol ($1' \rightarrow 2'$). H_2N-NH_3 is formed by the coupling of the NH_2 radical and one NH_3 molecule; this is an exergonic step that releases 19.3 kcal/mol of energy ($2' \rightarrow R2'\_3$). H_2N-NH_2 is then formed through the extraction of one hydrogen atom from each of the H_2N-NH_3 species, followed by H_2 desorption ($R2'\_3 \rightarrow R2, 2'\_4$). N_2 and H_2 are also formed from H_2N-NH_2 in a similar manner as in route 2 ($R2, 2'\_4 \rightarrow 5 \rightarrow 6$). The activation energy for H_2 and N_2 formation owing to NH_3 decomposition by route 2′ is estimated to be 65.8 kcal/mol.

3.4. *Discussion with comparisons*

According to the abovementioned results obtained from DFT calculations, the activation energies for the decomposition of NH_3 to N_2 and H_2 are 236 and 74.4 kcal/mol for routes 1 and 2, respectively. Route 2 is thus energetically more favorable than route 1. Hence, it is suggested that H_2 and N_2 are formed via H_2N-NH_2

formation owing to NH_3 decomposition. However, the required formation energies for H_2N-NH_2 as an intermediate are 20.8 and 7.8 kcal/mol in routes 2 and route 2′, respectively. Therefore, H_2N-NH_2 formation by the coupling of the NH_2 radical and one NH_3 molecule is thermodynamically favored. The result of DFT calculations indicates that the formation of N_2 occurs after H_2 formation. Hence, it is speculated that no detection of N_2 in the initial stage of the reaction for the MS measurements is due to the successive formation of N_2 from H_2N-NH_2 (see Fig. 3). The activation energies of the pathways are estimated to be 74.4 and 59.2 kcal/mol, respectively, not very different from each other. It is thus possible that NH_3 decomposition proceeds via both route 2 and route 2′.

4. Conclusions

This work showed that Ni/TiO_2 photocatalysts indicated the highest activity among various metal-loaded photocatalysts for the decomposition of NH_3 to N_2 and H_2. From the result of MS measurements, it was shown that the H_2 was formed by the photodecomposition of NH_3. ESR measurements indicated that the NH_2 radical was formed as an intermediate. To investigate the mechanism of NH_3 decomposition, three reaction pathways were proposed, in which N_2 and H_2 were formed with the help of an NH_2 radical: route 1 involved the formation of NH radicals through extraction of one hydrogen atom from each of two NH_2 radicals; route 2 involved the formation of NH_2-NH_2 by the coupling of adjacent NH_2 radicals; and finally, route 2′, involved the formation of NH_2-NH_2 via formation of H_2N-NH_3. The activation energies for routes 1 and 2 were estimated to be 236 kcal/mol and 74.8 kcal/mol, respectively. Route 2 was found to be more energetically favorable than route 1. Possible reaction pathways by which N_2 and H_2 were formed through NH_2-NH_2 coupling were further split into route 2, involving the formation of H_2N-NH_2 by coupling of NH_2 radicals, and route 2′, where NH_2 interacted with one NH_3 molecule in the gas phase. Their activation energies were estimated to be 74.4 kcal/mol and 59.2 kcal/mol, respectively, which were not significantly different from each other; therefore, it is possible that NH_3 decomposition proceeded by both routes 2 and 2′ via the formation of NH_2-NH_2. Ni^0 can be suggested to have enhanced the reaction pathways via H_2N-NH_2, because Ni^0 was present in the catalyst that showed a higher catalytic activity than the others. Our findings can serve as a reference for similar photodecomposition reactions, which might open up a new avenue to the design of more efficient catalytic systems.

References

[1] M. Anpo, H. Yamashita, S. Kawasaki, Y. Ichihashi, Sekiyu Gakkaishi 38 (1995) 300–310.
[2] M. Anpo, Y. Ichihashi, M. Takeuchi, H. Yamashita, Res. Chem. Intermed. 24 (1998) 143–149.
[3] A. Okemoto, K. Kishishita, S. Maeda, S. Gohda, M. Misaki, Y. Koshiba, K. Ishida, T. Horie, K. Taniya, Y. Ichihashi, S. Nishiyama, Appl. Catal. B: Environ. 192 (2016) 88–92.
[4] J. Wang, P. Rao, W. An, J. Xu, Y. Men, Appl. Catal. B: Environ. 195 (2016) 141–148.
[5] A.F. Alkaim, T.A. Kandielc, F.H. Husseind, R. Dillert, D.W. Bahnemanna, Appl. Catal. A: Gen. 466 (2013) 32.
[6] A. Cruz-López, A.C.L. Pozos, S.I.S. Vázqueza, R. Zanella, R. Gómez, Mater. Res. Bull. 83 (2016) 603–608.
[7] H. Yu, X. Huang, P. Wang, J. Yu, J. Phys. Chem. 120 (2016) 3722.
[8] B. Huang, M. Wey, J. Nanopart. Res. 16 (2014) 2178.
[9] V.A. Ogarev, V.M. Rudoi, O.V. Dement'eva, Russ. J. Phys. Chem. A 88 (2014) 181.
[10] M. Reli, M. Edelmannová, M. Šihor, P. Praus, L. Svoboda, K.K. Mamulová, H. Otoupalíková, L. Čapek, A. Hospodková, L. Obalová, K. Kočí, Int. J. Hydrog. Energy 37 (2012) 8530.
[11] R. Pelka, I. Moszyníska, W. Arabczyk, Catal. Lett. 128 (2009) 72.
[12] R. Pelka, W. Arabczyk, Top. Catal. 52 (2009) 1506.
[13] N. Itoh, A. Oshima, E. Suga, T. Sato, Catal. Today 236 (2014) 70.
[14] A. Klerke, S.K. Klitgaard, R. Fehrmann, Catal. Lett. 130 (2009) 541.

[15] K. Obata, K. Kishishita, A. Okemoto, K. Taniya, Y. Ichihashi, S. Nishiyama, Appl. Catal. B: Environ. 200 (2014) 160–161.
[16] H. Yamashita, M. Honda, M. Harada, Y. Ichihashi, M. Anpo, T. Hirano, N. Itoh, N. Iwamoto, J. Phys. Chem. B 102 (1998) 10707–10711.
[17] R. Pol, M. Guerrerob, E. García-Lecinac, A. Altubec, E. Rossinyold, S. Garronie, M.D. Barób, J. Ponsa, J. Sortf, E. Pellicerb, Appl. Catal. B: Environ. 181 (2016) 270.
[18] K. Siwinska-Stefanska, B. Kurc, J. Power Sources 299 (2015) 286.
[19] Y. Lin, C. Weng, H. Hsu, Y. Lin, C. Shiesh, Int. J. Photoenergy 1 (2013).
[20] L. Yang, M. Gao, B. Dai, X. Guo, Z. Liu, B. Peng, Appl. Surf. Sci. 386 (2016) 337.
[21] Y. Zou, S. Kang, X. Li, L. Qin, J. Mu, Int. J. Hydrog. Energy 39 (2014) 15403.
[22] Y. Luan, L. Jing, M. Xie, X. Shi, X. Fan, Y. Cao, Y. Feng, Phys. Chem. Chem. Phys. 14 (2012) 1352.
[23] D. Ponnusamy, S. Madanagurusamy, J. Electron. Mater. 44 (2015) 4726.
[24] M. Zalfani, B. van der Schueren, M. Mahdouani, R. Bourguiga, W. Yu, M. Wu, O. Deparis, Y. Li, B. Su, Appl. Catal. B: Environ. 199 (2016) 187.
[25] M. Xing, D. Qi, J. Zhang, F. Chen, B. Tian, S. Bagwas, M. Anpo, J. Catal. 294 (2012) 37–46.
[26] J. Nemoto, N. Gokan, H. Ueno, M. Kaneko, J. Photochem. Photobiol. A: Chem. 185 (2007) 295–300.
[27] Z. Li, S. Chen, S. Gong, B. Feng, Z. Zhou, Comp. Theor. Chem. 1088 (2016) 24–31.
[28] G. Zhao, H. Liu, D. Zhang, Xu. Huang, X. Yang, ACS Catal. 4 (2014) 2231.
[29] S. Lin, Y. Pei, J. Phys. Chem. C 118 (2014) 20346.
[30] L. Liu, Y. Wu, T. Wang, X. Gao, J. Zhu, Y. Zhao, J. Org. Chem. 79 (2014) 5074.
[31] Q. Lu, H. Yu, Y. Fu, J. Am. Chem. Soc. 136 (2014) 8252.
[32] C. Miao, B. Wang, Y. Wang, C. Xia, Y. Lee, W. Nam, W. Sun, J. Am. Chem. Soc. 138 (2016) 936.
[33] S. Kim, J.W. Ginsbach, J.Y. Lee, R.L. Peterson, J.J. Liu, M.A. Siegler, A.A. Sarjeant, E.I. Solomon, K.D. Karlin, J. Am. Chem. Soc. 137 (2015) 2867.
[34] H. Yamashita, M. Harada, J. Misaka, M. Takeuchi, Y. Ichihashi, F. Goto, M. Ishida, T. Sasaki, M. Anpo, J. Synchrotron Radiat. 8 (2001) 569–571.
[35] V.P. Indrakanti, J.D. Kubicki, H.H. Schobert, Energy Fuels 22 (2008) 2611.
[36] I. Onal, S. Soyer, S. Senkan, Surf. Sci. 600 (2006) 2457.
[37] R. Wanbayor, V. Ruangpornvisuti, J. Mol. Struct. THEOCHEM 952 (2010) 103.
[38] J. Guan, P. Duffy, J.T. Carter, D.P. Chong, J. Chem. Phys. 98 (1993) 4753–4765.
[39] V. Zunic, S.D. Skapin, D. Suvorov, J. Am. Ceram. Soc. 98 (2015) 2997.
[40] Y. Gönüllü1, A.A. Haidry, B. Saruhan, Sens. Actuators B 217 (2015) 78.
[41] S. Ozkan, A. Mazare, P. Schmuki, Electrochim. Acta 176 (2015) 819.
[42] S. Sitthisa, W. An, D.E. Resasco, J. Catal. 284 (2011) 90.
[43] L. Qin, J. Xu, J. Lian, Z. Jiang, Q. Jiang, Surf. Coat. Technol. 203 (2008) 142.
[44] A. Kumara, J.T. Miller, A.S. Mukasyan, E.E. Wolf, Appl. Catal. A: Gen. 467 (2013) 593.
[45] S. Yamazoe, T. Okumura, T. Tanaka, Catal. Today 120 (2007) 220.
[46] H. Yuzawa, T. Mori, H. Itoh, H. Yoshida, J. Phys. Chem. C 116 (2012) 4126.
[47] F. Köksal, O. Çakir, İ. Gümrükçü, M. Birey, Z. Naturforsch. 40a (1985) 903.